Thermodynamic properties of a weakly modulated graphene monolayer in a magnetic field

2010 J. Phys.: Condens. Matter 22 025503

(http://iopscience.iop.org/0953-8984/22/2/025503)

IOP Publishing Journal of Physics: Condensed Matter

J. Phys.: Condens. Matter **22** (2010) 025503 (9pp) doi:10.1088/0953-8984/22/2/025503

Thermodynamic properties of a weakly modulated graphene monolayer in a magnetic field

R Nasir[1], M A Khan[1], M Tahir[2] and K Sabeeh[1,3]

[1] Department of Physics, Quaid-i-Azam University, Islamabad 45320, Pakistan
[2] Department of Physics, University of Sargodha, Sargodha 40100, Pakistan

E-mail: ksabeeh@qau.edu.pk

Received 8 September 2009, in final form 3 November 2009
Published 14 December 2009
Online at stacks.iop.org/JPhysCM/22/025503

Abstract

Theoretical investigation of thermodynamic properties of an electrically modulated graphene monolayer in the presence of a perpendicular magnetic field B is presented. This work is aimed at determining the modulation-induced effects on the thermodynamic properties of graphene. The results obtained are compared with those of conventional two-dimensional electron gas (2DEG) systems realized in semiconductor heterostructures. The one-dimensional periodic potential, due to electric modulation lifts the degeneracy of the Landau levels and converts them into bands whose width oscillates as a function of B. We find commensurability (Weiss) oscillations for small values of B and de Haas–van Alphen (dHvA)-type oscillations at larger values of B. We find that the modulation-induced effects on the thermodynamic properties are enhanced and less damped with temperature in graphene compared with conventional 2DEG systems. Furthermore, we have derived analytic asymptotic expressions which allow us to determine the critical temperature and critical magnetic field for the damping of magnetic oscillations in the thermodynamic quantities considered here.

(Some figures in this article are in colour only in the electronic version)

1. Introduction

Monolayer graphene is a two-dimensional (2D) honeycomb lattice of carbon atoms. Its experimental realization has opened up new horizons in the field of condensed matter physics and materials science. Unique electronic properties of graphene make it substantially different from conventional two-dimensional electron gas (2DEG) systems realized in semiconductor heterostructures. The quasiparticles in graphene at low energies have a linear dispersion relation $\varepsilon_k = \hbar v_F k$ with a characteristic velocity of $v_F = 10^6$ m s^{-1} [1]. These quasiparticles, called massless Dirac fermions, can be treated as electrons with zero mass. The fact that charge carriers in graphene can be described by a Dirac-like equation, rather than the usual Schrödinger equation for nonrelativistic quantum particles in conventional 2DEG, can be seen as a consequence of graphene's crystal structure. This consists of two equivalent carbon sublattices. Quantum-mechanical hopping between the sublattices leads to the formation of two energy bands, and their interaction near the Brillouin zone yields the conical energy spectrum. In contrast, electrons in conventional 2DEG systems are confined in one dimension but are free in the other two, resulting in parabolic dispersion in two dimensions. As a result of this difference in the energy spectrum, one can expect that quasiparticles in graphene behave differently from those in conventional 2DEG systems. The zero mass property of charge carriers in graphene along with charge conjugation symmetry results in many unusual transport phenomena such as the anomalous quantum Hall effect, Klein tunneling and a non-zero Berry phase [2–5]. Currently, there is great interest in exploring the electronic properties of graphene in the presence of nonuniform potentials, such as in p–n junctions [6], as well as in periodic potentials. The effects of a periodic potential on the electron properties of 2D systems have been the subject of continued interest, where electrical modulation of the 2D

[3] Author to whom any correspondence should be addressed.

system can be carried out by depositing an array of parallel metallic strips on the surface or through two interfering laser beams [7]. More recently in graphene, electrostatic [8] and magnetic [9] periodic potentials have been shown to modulate its electronic structure in unique ways, leading to fascinating physics and possible applications. Periodic potentials are induced in graphene by interaction with a substrate [10] or controlled adatom deposition [11]. In this context, it was recently shown [10] that epitaxial graphene on an Ir(111) substrate induces a weak periodic potential in graphene. In addition, it was shown that periodic ripples in suspended graphene also induce a periodic potential in a perpendicular electric field [12]. Epitaxial growth of graphene on top of a prepatterned substrate is also a possible route to modulation of the potential experienced by the electrons. In this work, we complement these recent studies to discuss the effects of a weak electric modulation on the thermodynamic properties of a graphene monolayer subjected to an external magnetic field perpendicular to the graphene plane. Electric modulation, in addition to the applied magnetic field, introduces two new length scales in the system, a period of modulation and cyclotron radius at the Fermi energy, the commensurability of these length scales giving rise to interesting physical effects on the thermodynamic response. It was found earlier that commensurability (Weiss) oscillations [7] appear in magnetoresistance when conventional 2DEG is subjected to artificially created periodic potentials (either electric or magnetic). These oscillations were found to be the direct consequence of the commensurability of the two length scales mentioned above: the cyclotron orbit radius $R_c = \sqrt{2\pi n_e} l^2$ (where n_e is the density of electrons and $l = \sqrt{\hbar/eB}$ is the magnetic length) and the period of modulation a. In this work, we not only investigate the effects of electrical modulation on the thermodynamic properties of a graphene monolayer but also compare our results with the previously obtained results for conventional 2DEG systems found in semiconductor heterostructures [13, 14].

This paper is arranged as follows. In section 2, we give the formulation of the problem. Calculation of the thermodynamic quantities is given in section 3 and numerical results are discussed in section 4. Numerical results are supported by analytical results derived in the asymptotic limit; these are presented in section 5.

2. Formulation

We consider a graphene monolayer in the xy plane subjected to a magnetic field B along the z direction. In the Landau gauge, the unperturbed single-particle Dirac-like Hamiltonian may be written as [3–5, 12]

$$H_o = v_F \boldsymbol{\sigma} \cdot (-i\hbar\nabla + e\mathbf{A}). \tag{1}$$

Here, $\boldsymbol{\sigma} = \{\sigma_x, \sigma_y\}$ are the Pauli matrices and $v_F = 10^6$ m s^{-1} characterizes the electron velocity with $\mathbf{A} = (0, Bx, 0)$ the vector potential. The normalized eigenfunctions of the Hamiltonian given in equation (1) are

$$\Psi_{n,k_y} = \frac{e^{ik_y y}}{\sqrt{2L_y l}} \begin{pmatrix} -i\phi_{n-1}[(x+x_o)/l] \\ \phi_n[(x+x_o)/l] \end{pmatrix}, \tag{2}$$

where $\phi_n = \frac{\exp(-x^2/2)}{\sqrt{2^n n!\sqrt{\pi}}} H_n(x)$, $H_n(x)$ are the Hermite polynomials, L_y is the normalization length in the y direction, n is an integer corresponding to the Landau level index and $x_o = k_y l^2$ is the center of the cyclotron orbit. The energy eigenvalues are

$$\varepsilon_n = \sqrt{n}\hbar\omega_g, \tag{3}$$

where $\omega_g = v_F\sqrt{\frac{2eB}{\hbar}}$ is the cyclotron frequency of the Dirac electrons in graphene. In order to investigate the effects of modulation, we express the Hamiltonian in the presence of modulation as

$$H = H_o + U(x). \tag{4}$$

Here, $U(x)$ is the one-dimensional periodic modulation potential along the x axis and is given by

$$U(x) = V_o \cos Kx. \tag{5}$$

$K = \frac{2\pi}{a}$, a is the period of modulation and V_o is the constant modulation amplitude. To account for weak modulation we take V_o to be an order of magnitude smaller than the Fermi energy $\varepsilon_F = v_F\hbar k_F$, where $k_F = \sqrt{2\pi n_e}$ is the magnitude of the Fermi wavevector with n_e the density of electrons. This allows us to apply standard first-order perturbation theory to determine the energy eigenvalues in the presence of modulation. The first-order energy correction is

$$\varepsilon_{n,x_o} = \varepsilon_n + |V_n| \cos Kx_o. \tag{6}$$

Here, $|V_n| = \frac{V_o}{2}\exp(-\frac{u}{2})[L_n(u) + L_{n-1}(u)]$, $u = \frac{K^2 l^2}{2}$, and $L_n(u)$ and $L_{n-1}(u)$ are Laguerre polynomials. It is important to mention that we have taken the Fermi level in this system to be upshifted from the Dirac point, which indicates that this model relates to n-doped graphene. For undoped graphene, the Fermi level will be at the Dirac point and the density of electrons in the conduction band in turn will be zero. However, real graphene samples are usually doped or can easily be doped by different methods [19]. To carry over the calculation performed below to p-doped graphene, where the Fermi energy is downshifted from the Dirac point, all we have to do is substitute $-\varepsilon$ for ε, $-\omega_g$ for ω_g and the Fermi Dirac distribution function of holes, $1 - f(\varepsilon)$, for that of electrons, $f(\varepsilon)$, in the expressions given below. Both the density of states, $D(\varepsilon)$, and the Helmholtz free energy, F, expressions turn out to be the same as that of the n-type system. Therefore, our results are valid for p-doped graphene as well.

Although similar features in the energy spectrum have also been found in the 2DEG system there are substantial differences between the two spectra. The Landau level spectrum of Dirac electrons depends on the square root of both the magnetic field B and the Landau band index n against linear dependence in the case of standard electrons in conventional 2DEG. The energy eigenvalues in the presence of modulation given by equation (6) contain a term which is a linear combination of two successive Laguerre polynomials with indices n and $n-1$, whereas standard electrons in 2DEG obey a relation containing a single Laguerre polynomial with index n.

We find that the modulation potential lifts the degeneracy of the Landau levels and broadens the formerly sharp levels into electric Landau bands. Further, electric-modulation-induced broadening of the energy spectrum is nonuniform. The Landau bandwidth V_n oscillates as a function of n since $L_n(u)$ is an oscillatory function of the index n. Landau bands become flat for those values of B for which the modulation strength becomes zero. By putting $V_n = 0$, one can obtain the flat band condition:

$$\exp\left(-\frac{u}{2}\right)[L_n(u) + L_{n-1}(u)] = 0. \tag{7}$$

Applying the asymptotic expression [15]:

$$\exp\left(-\frac{u}{2}\right)L_n(u) \simeq \frac{1}{\sqrt{\pi\sqrt{nu}}}\cos\left(2\sqrt{nu} - \frac{\pi}{4}\right) \tag{8}$$

with $L_n(u) = L_{n-1}(u)$, one obtains from equations (7) and (8) the following condition:

$$2R_c = a(i - 1/4), \qquad i = 1, 2, 3, \ldots, \tag{9}$$

where $R_c = k_F l^2$ is the classical cyclotron orbit. From equations (6) and (8) it can be observed that, in the large n limit, electron bandwidth oscillates sinusoidally and is periodic in $1/B$, for fixed values of n and a. When n is small, the bandwidth still oscillates, but the condition (9) no longer holds because neither equation (8) nor $L_n(u) \simeq L_{n-1}(u)$ is valid. Interestingly, for low values of B, when many Landau levels are filled, both the graphene and 2DEG systems have the same flat band condition [13, 14].

It is well known that, in the absence of modulation, the density of states (DOS) consists of a series of delta functions at energies equal to ε_n. The addition of a weak periodic electric modulation, however, modifies the former delta functions leading to DOS broadening. The density of states $D(\varepsilon)$ is given by [16]

$$D(\varepsilon) = \frac{A}{\pi l^2}\sum_{n,x_o}\delta(\varepsilon - \varepsilon_{n,x_o}) = \frac{A}{\pi l^2}\sum_n \frac{\theta(|V_n| - |\varepsilon - \varepsilon_n|)}{\sqrt{|V_n|^2 - (\varepsilon - \varepsilon_n)^2}}, \tag{10}$$

where $\theta(x)$ is the Heaviside unit step function and A is the area of the sample.

Before we begin the calculation of equilibrium thermodynamic quantities, it is necessary to discuss the regime of validity of the perturbation theory presented above. For large n the level spacing given by equation (3) goes as $\omega_g(\sqrt{n} - \sqrt{(n-1)}) \longrightarrow \omega_g \frac{1}{2\sqrt{n}}$ and the width of the nth level goes as $2\omega_o n^{1/2}$, apart from the modulation. There is therefore a value of n at which the width becomes equal to the spacing and the perturbation theory is no longer valid. This occurs when $n_{\max} = \frac{1}{16V_o^4}\pi^2 u(\hbar\omega_g)^4 = \frac{\pi^4}{2\hbar a^2 V_o^4} v_F^4 eB$. For a fixed electron density and the period of modulation this suggests the minimum value for the magnetic field B below which it is necessary to carry out a more sophisticated analysis. Note that this argument applies to any other calculation which treats the modulation as a perturbation. Furthermore, dispersion of charge carriers in graphene is found to be essentially linear within ± 1 eV of the Fermi energy [1–5]. Since, in this work, we limit ourselves to low temperatures and weak magnetic fields as well as weak modulation, the assumption of linear dispersion is expected to hold.

3. Equilibrium thermodynamic quantities

In this section, we determine the electronic contribution to the equilibrium thermodynamic properties of a graphene monolayer subjected to a perpendicular magnetic field and weak electric modulation. To facilitate comparison with results for a 2DEG, we compute the following thermodynamic quantities: chemical potential, Helmholtz free energy, electronic specific heat, orbital magnetization and orbital magnetic susceptibility.

The magnetic field (B)-and temperature (T)-dependent chemical potential $\mu \equiv \mu(B, T)$ of a system can be determined by inverting the following relation:

$$N = \int_0^\infty D(\varepsilon) f(\varepsilon)\, \mathrm{d}\varepsilon. \tag{11}$$

Here, the Fermi Dirac distribution function $f(\varepsilon) = [\exp(\frac{\varepsilon - \mu}{k_B T}) + 1]^{-1}$, k_B is the Boltzmann constant and N is the total number of electrons. The total internal energy U is given as

$$U = \int_0^\infty \varepsilon D(\varepsilon) f(\varepsilon)\, \mathrm{d}\varepsilon. \tag{12}$$

We observe that $\mu(B, T)$ is affected by changes in $D(\varepsilon)$. Substituting equation (10) into equation (11), we obtain

$$N = \frac{A}{\pi^2 l^2}\sum_{n=0}^{\infty}\int_{-1}^{1}\frac{\mathrm{d}x}{\sqrt{1 - x^2}}(1 + \alpha_n \exp[z_n x])^{-1}. \tag{13}$$

Here $x = \frac{|\varepsilon - \varepsilon_n|}{|F_n|}$, $\alpha_n = \exp[\frac{\varepsilon_n - \mu}{k_B T}]$ and $z_n = |V_n|/(k_B T)$. Equation (13) can be applied to both modulated and unmodulated systems ($z_n \equiv 0$). For fixed electron concentration $n_e = N/A$ the above equation gives $\mu(B, T)$ only implicitly and it cannot be decoupled explicitly. Therefore, we have solved equation (13) numerically to obtain chemical potential $\mu(B, T)$. Once the chemical potential and the density of states are known, the free energy F of the system can be calculated. From there on the thermodynamic properties of the system can be obtained from the free energy by taking the appropriate derivatives. For a system of non-interacting fermions, the Helmholtz free energy is given by [17]

$$F = \mu N - k_B T\int_0^\infty D(\varepsilon)\ln\left[1 + \exp\left(\frac{\mu - \varepsilon}{k_B T}\right)\right]\mathrm{d}\varepsilon. \tag{14}$$

The density of states $D(\varepsilon)$ is the central quantity in the above expression. The expression for $D(\varepsilon)$ in graphene is different from that in conventional 2DEG due to the difference in the energy spectrum in the two cases. This difference will be reflected in the thermodynamic properties of the two systems. The free energy for an electrically modulated graphene system is given as

$$F = \mu N - k_B T\frac{A}{\pi^2 l^2}\sum_{n=0}^{\infty}\int_{-1}^{1}\frac{\mathrm{d}x}{\sqrt{1 - x^2}} \times \ln[1 + \alpha_n^{-1}\exp(-z_n x)]. \tag{15}$$

From equation (15), we calculate the electronic contribution to the entropy $S = (U - F)/T$ and the electronic specific

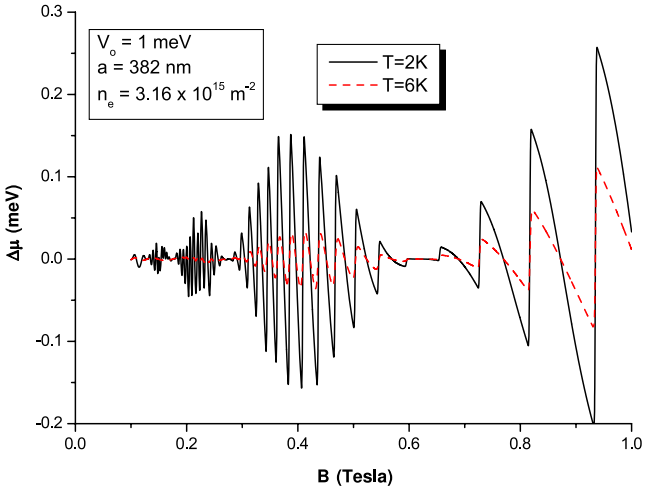

Figure 1. The change in the chemical potential ($\Delta\mu$) due to 1D modulation versus magnetic field B at two different temperatures 2 K (solid curve) and 6 K (broken curve).

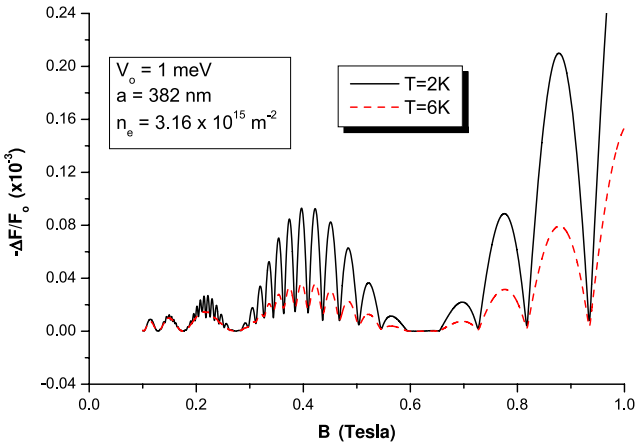

Figure 2. The change in the free energy ($-\Delta F$) versus magnetic field B at two different temperatures 2 K (solid) and 6 K (broken). The y axis has been scaled using $F_o = N\varepsilon_F/2$ so that it appear dimensionless.

heat $C = -T(\frac{\partial^2 F}{\partial T^2})_{A,N}$. The orbital motion of the electrons in the presence of an external magnetic field gives rise to the electronic contribution to the orbital magnetization $M = -(\frac{\partial F}{\partial B})_{A,N}$ as well as orbital magnetic susceptibility $\chi = -(\partial^2 F/\partial B^2)_{A,N}$. These quantities are numerically evaluated and the results presented in section 4.

4. Results and discussion

Numerical results for thermodynamic properties of a graphene monolayer subjected to electrical modulation and an external magnetic field are presented. The focus, here, is on the modulation-induced changes in the thermodynamic properties. To facilitate comparison with a 2DEG system we have chosen the following parameters: $n_e = N/A = 3.16 \times 10^{15}$ m^{-2} and $a = 382$ nm. The strength of the electrical modulation is taken to be $V_o = 1$ meV. These are the same parameters considered for a 2DEG in [13, 14]. Modulation-induced effects on thermodynamic quantities can be highlighted by calculating the difference between the modulated case and the unmodulated case in each system.

In figures 1–5, we have plotted the change in various thermodynamic properties due to electric modulation at temperatures of $T = 2$ K (solid curve) and $T = 6$ K (broken curve).

In figure 1, we have plotted the change in chemical potential versus magnetic field at temperatures 2 K (solid) and 6 K (broken). For a conventional 2DEG system, for $B < 0.3$ T, oscillations depend very weakly on temperature, which is a clear signature of Weiss-type oscillations whereas, for $B > 0.3$ T, the oscillations depend strongly on temperature, in particular they die out at 6 K, a clear signature of dHvA-type oscillations. Furthermore, the zeros in the chemical potential are in close agreement with those predicted by the flat band condition equation (9). We have discussed this point from the perspective of the bandwidth in the discussion of figure 2 given below. In graphene, the value of B defining the

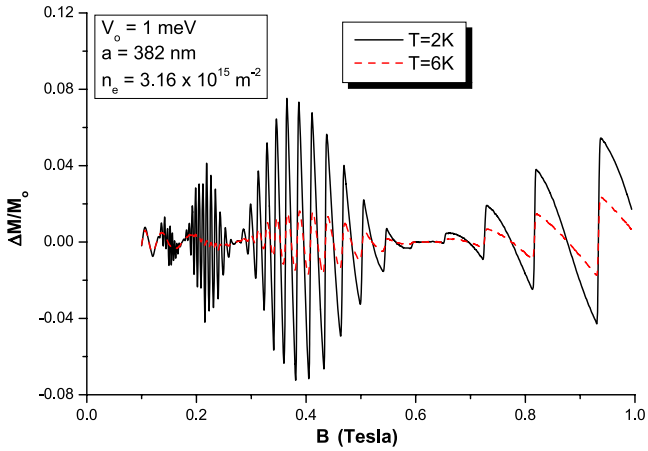

Figure 3. The change in the orbital magnetization (ΔM) versus magnetic field B at two different temperatures 2 K (solid) and 6 K (broken). The y axis has been scaled using $M_o = N\mu_B$ so that it appear dimensionless.

boundary between the two oscillatory phenomena is quite low (it lies somewhere between 0.1 and 0.15 T). For smaller values of B, Weiss-type oscillations are present and the amplitude of the oscillations remains essentially the same at different temperatures. For larger values of B, the familiar dHvA-type oscillations are present, with the amplitude of oscillations reduced considerably at comparatively higher temperatures. dHvA oscillations are found to start at a lower magnetic field in graphene compared to 2DEG. This difference can be attributed to the large cyclotron gap in graphene compared to the cyclotron gap of conventional 2DEG systems since the condition $\hbar\omega_g \gg k_B T$ is satisfied at lower magnetic fields in graphene compared to a 2DEG. Furthermore, in a conventional 2DEG system oscillations completely die out at 6 K whereas they persist in graphene at this temperature. In section 4 of the present paper, we have derived analytic asymptotic expressions for the free energy in order to obtain temperature scales for both dHvA-type and Weiss-type oscillations. Our

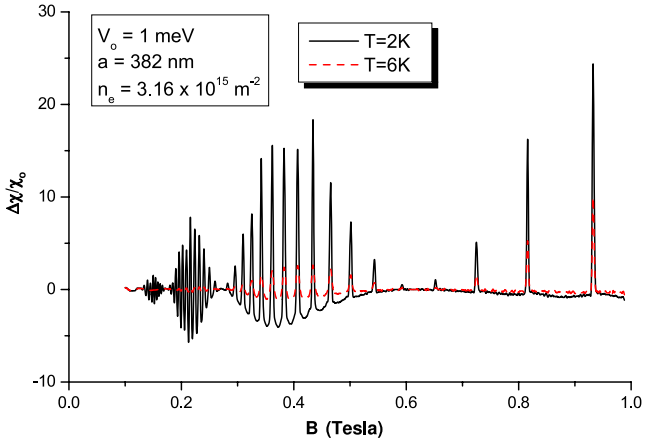

Figure 4. The change in the magnetic susceptibility ($\Delta\chi$) versus magnetic field B at two different temperatures 2 K (solid) and 6 K (broken). The y axis has been scaled using $\chi_o = N\mu_B/B$ so that it appears dimensionless.

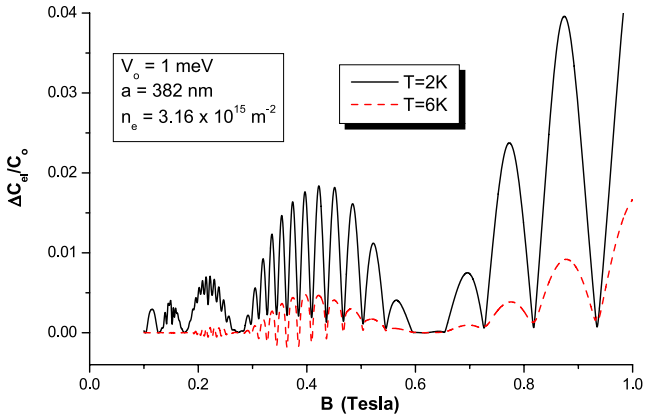

Figure 5. The change in the specific heat $\Delta C_{el}/C_o$ versus magnetic field B at two different temperatures 2 K (solid) and 6 K (broken). The y axis has been scaled using $C_o = Nk_B$ so that it appears dimensionless.

findings show that for a graphene system comparatively higher temperatures are required for the damping of both the dHvA- and Weiss-type oscillations. This result holds for all the thermodynamic quantities considered here.

The free energy for the two systems is shown in figure 2. To make the y axis dimensionless, the free energy has been scaled using $F_o = \frac{1}{2}N\varepsilon_F$. It can be seen that at small values of B modulation induces weakly temperature-dependent Weiss-type oscillations occur, with zeros occurring at their respective flat band conditions. To illustrate this point, we consider the bandwidth of the nth Landau band which is given by $V_o \exp[-u/2]|L_n(u) + L_{n-1}(u)|$. For the modulation-induced effects considered here the magnetic field is small and in order to make an estimate of the minima of the bandwidth we take the large n limit of the Laguerre polynomial term such that $\exp[-u/2]L_n(u)$ may be approximated by $(\pi^2 nu)^{-1/4}\cos(2\sqrt{nu} - \pi/4)$. If the bandwidth is plotted in both cases, for the exact result and the asymptotic limit, minima of the bandwidth are found at $B = 0.086, 0.106, 0.140, 0.184, \ldots$. Modulation-induced change in free energy vanishes at $B = 0.084, 0.102, 0.130, 0.174, \ldots$ which shows that the vanishing of the change in free energy occurs at those values of the magnetic field where the bandwidth minima occur.

Furthermore, Weiss oscillations are more pronounced in the graphene system; significantly the amplitude of Weiss oscillations for the graphene system remains unchanged at higher temperature, contrary to the 2DEG in which damping is observed. The familiar dHvA-type oscillations are observed for higher values of B. As in the case of the chemical potential, the dHvA-type oscillations start quite early. The first period for the dHvA-type oscillations starts at $B = 0.3$ T and extends up to 0.6 T for the conventional 2DEG system, whereas for graphene the first period of dHvA oscillations starts at $B = 0.175$ T and terminates at 0.27 T.

In figures 3 and 4 we have plotted the changes in the magnetization ΔM and the susceptibility $\Delta\chi$ against the magnetic field. The change in orbital magnetization and change in susceptibility has been scaled using $M_o = N\mu_B$ and $\chi_o = N\mu_B/B$, respectively, where $\mu_B = e\hbar v_F^2/(2\varepsilon_F) = 5.021$ meV T^{-1} is the effective Bohr magneton in graphene, such that the y axis in both curves appears dimensionless. The orbital magnetization considered here is the Landau diamagnetic contribution. As the magnetic field is applied, the electron distribution breaks up into a series of Landau levels. This change in energy with field is equivalent to magnetization of a system. At low B, Weiss-type oscillations are clearly visible while, for higher values of B, dHvA oscillations are present. The Weiss oscillations are weakly dependent on temperature while the dHvA type are strongly affected. We observe that dHvA oscillations in ΔM and $\Delta\chi$ are less damped with temperature in the graphene system than in the 2DEG system.

In figure 5, we plot the change in the electronic specific heat capacity against the magnetic field. The y axis has been scaled using $C_o = Nk_B$ to appear dimensionless. We find that the amplitude of the Weiss-type oscillations in $\frac{\Delta C_{el}}{C_o}$ is not large, which suggests that the modulation-induced effects on the specific heat are small. We also find that specific heat at low B is enhanced when the modulation is introduced compared to the situation without modulation. This occurs due to the broadening of the Landau levels caused by the modulation resulting in the contribution of intra-Landau level thermal excitations to the electronic specific heat in addition to the contribution from inter-Landau level thermal excitations. We also observe damping with temperature of the dHvA-type oscillations at higher B. In order to gain further physical insight into the results presented above, we analyze asymptotic expressions of the thermodynamic quantities in section 5.

5. Asymptotic results

In this section we will derive an analytic expression for the Helmholtz free energy, which is true in the quasi-classical limit when many Landau bands are filled. To obtain the asymptotic expression for the Helmholtz free energy it is essential to first derive an asymptotic expression for the density of states. In the

quasi-classical case, an approximate analytical formula for the density of states is given in the appendix as

$$D(\varepsilon) = \frac{A}{\pi l^2}\frac{\varepsilon}{(\hbar\omega_g)^2}\left[1 + 2\cos\left(\frac{2\pi\varepsilon^2}{(\hbar\omega_g)^2}\right) \times \left\{1 - \Omega\varepsilon\cos^2\left(\sqrt{2}\frac{\varepsilon}{\hbar\omega_g}Kl - \frac{\pi}{4}\right)\right\}\right], \tag{16}$$

where

$$\Omega = V^2\frac{a}{l}\left(\frac{\sqrt{2}}{\hbar\omega_g}\right)^3.$$

The density of states consists of two parts, with the terms outside the curly braces being just those corresponding to the unmodulated case, in the limit of vanishing modulation potential. The additional modulation contribution to the density of states depends quadratically on the strength of modulation through Ω in equation (16). Substitution of equation (16) in equation (14) yields

$$F \approx \mu N - \frac{A}{\pi l^2}\frac{k_B T}{(\hbar\omega_g)^2}\int_0^\infty \varepsilon\left\{1 + 2\cos\left(\frac{2\pi\varepsilon^2}{(\hbar\omega_g)^2}\right)\right\} \times \ln\left[1 + \exp\left(\frac{\mu - \varepsilon}{k_B T}\right)\right]\mathrm{d}\varepsilon + \Omega\frac{A}{\pi l^2}\frac{k_B T}{(\hbar\omega_g)^2}\int_0^\infty \varepsilon^2\cos\left(\frac{2\pi\varepsilon^2}{(\hbar\omega_g)^2}\right) \times \cos^2\left(\sqrt{2}\frac{\varepsilon}{\hbar\omega_g}Kl - \frac{\pi}{4}\right)\ln\left[1 + \exp\left(\frac{\mu - \varepsilon}{k_B T}\right)\right]\mathrm{d}\varepsilon. \tag{17}$$

The first two terms on the right-hand side correspond to the unmodulated free energy F_u while the third term gives the modulation contribution to the Helmholtz free energy $F_{mod} \equiv \Delta F$. Firstly, we consider F_u:

$$F_u = \mu N - \frac{A}{\pi l^2}\frac{k_B T}{(\hbar\omega_g)^2}\int_0^\infty \varepsilon\left\{1 + 2\cos\left(\frac{2\pi\varepsilon^2}{(\hbar\omega_g)^2}\right)\right\} \times \ln\left[1 + \exp\left(\frac{\mu - \varepsilon}{k_B T}\right)\right]\mathrm{d}\varepsilon. \tag{18}$$

Setting $(\varepsilon - \mu)/k_B T = 2\theta$. At low temperatures, such that μ coincides with the Fermi energy ε_F and $\varepsilon_F/k_B T \gg 1$, the above equation can be expressed as

$$F_u \approx \mu N - \frac{A}{\pi l^2}\frac{2(k_B T)^2\varepsilon_F}{(\hbar\omega_g)^2} \times \int_{-\varepsilon_F/2k_B T}^\infty \ln[1 + \exp(-2\theta)]\,\mathrm{d}\theta - \frac{A}{\pi l^2}\frac{4(k_B T)^2\varepsilon_F}{(\hbar\omega_g)^2}\int_{-\varepsilon_F/2k_B T}^\infty \cos\left(\frac{2\pi\varepsilon_F^2}{(\hbar\omega_g)^2} + \frac{8\pi k_B T\varepsilon_F}{(\hbar\omega_g)^2}\theta\right) \times \ln[1 + \exp(-2\theta)]\,\mathrm{d}\theta. \tag{19}$$

The second integral in the above equation is an integral of the type

$$I(\alpha, \beta; \theta_o) = \int_{-\theta_o}^\infty \cos(\alpha\theta + \beta)\ln[1 + \exp(-2\theta)]\,\mathrm{d}\theta,$$

where $\alpha = \frac{8\pi k_B T\varepsilon_F}{(\hbar\omega_g)^2}$, $\beta = \frac{2\pi\varepsilon_F^2}{(\hbar\omega_g)^2}$ and $\theta_o = \varepsilon_F/2k_B T \gg 1$. This integral can be performed analytically in the limit of large θ_o. Twice integrating by parts, followed by replacement of the lower limit of integration by $-\infty$, since $(\theta_o \gg 1)$, leads to

$$I(\alpha, \beta; \theta_o) \approx -\frac{2\theta_o}{\alpha}\sin(\beta - \alpha\theta_o) + \frac{2}{\alpha^2}\cos(\beta - \alpha\theta_o) - \frac{1}{\alpha^2}\int_{-\infty}^\infty \frac{\cos(\alpha\theta + \beta)}{\cosh^2(\theta)}\,\mathrm{d}\theta.$$

Using the following identity [15]:

$$\int_0^\infty \frac{\cos(\alpha\theta + \beta)}{\cosh^2(\gamma\theta)}\,\mathrm{d}\theta = \frac{\pi\alpha}{2\gamma^2\sinh(\frac{\pi\alpha}{2\gamma})}$$

we obtain

$$\int_{-\infty}^\infty \frac{\cos(\alpha\theta + \beta)}{\cosh^2(\theta)}\,\mathrm{d}\theta = \frac{\pi\alpha\cos(\beta)}{\sinh(\frac{\pi\alpha}{2})}$$

with the result

$$F_u \approx \mu N - \frac{A}{\pi l^2}\frac{2(k_B T)^2\varepsilon_F}{(\hbar\omega_g)^2} \times \int_{-\varepsilon_F/2k_B T}^\infty \ln[1 + \exp(-2\theta)]\,\mathrm{d}\theta - \frac{A}{\pi l^2}\frac{\varepsilon_F}{2\pi}\sin\left(\frac{2\pi\varepsilon_F^2}{(\hbar\omega_g)^2}\right) - \frac{A}{\pi l^2}\frac{(\hbar\omega_g)^2}{8\pi^2\varepsilon_F}\cos\left(\frac{2\pi\varepsilon_F^2}{(\hbar\omega_g)^2}\right) + \frac{A}{2\pi l^2}\frac{k_B T}{\sinh(T/T_g^{dHvA})}\cos\left(\frac{2\pi\varepsilon_F^2}{(\hbar\omega_g)^2}\right). \tag{20}$$

$T_g^{dHvA} = (\hbar\omega_g)^2/4\pi^2 k_B\varepsilon_F$, in the above expression, defines the critical temperature for dHvA-type oscillations in graphene and determines the amplitude of these oscillations at small magnetic fields. The point worth mentioning is that the critical temperature $T_{2DEG}^{dHvA} = \hbar\omega_c/2\pi^2 k_B$ for dHvA oscillations in the case of conventional 2DEG [13] is lower than the critical temperature for graphene. Further, the ratio is found to be independent of the external magnetic field such that

$$\frac{T_g^{dHvA}}{T_{2DEG}^{dHvA}} = \frac{v_F m_e}{\hbar\sqrt{2\pi n_e}} \approx 4. \tag{21}$$

The comparatively higher value of critical temperature found in graphene can be attributed to the larger cyclotron gap $\hbar\omega_g$, characteristic of Dirac fermions in graphene. Moreover, the effective mass term in T_{2DEG}^{dHvA} is analogous to the ε_F/v_F^2 (similar to the $E = m^*c^2$) term in T_g^{dHvA}, which also confirms the relativistic nature of Dirac fermions in graphene. Moreover, we find in equation (20) a pure oscillatory dHvA-type contribution to F_u due to the magnetic-field-dependent sine and cosine terms is present. If we compare the above result with the results for conventional 2DEG systems [13], we find that additional temperature-independent and magnetic-field-dependent sine and cosine terms are present in the expression for graphene. Furthermore, at higher temperatures, the last term on the right-hand side of equation (20) decays exponentially whereas the additional magnetic-field-dependent sine and cosine terms persist, contrary to the conventional 2DEG system.

Along the same lines, the second integral on the right-hand side of equation (17) may be solved for $F_{\rm mod} \equiv \Delta F$:

$$F_{\rm mod} = \Delta F = \Omega \frac{A}{\pi l^2} \frac{\varepsilon_{\rm F}^2}{2\pi} \left\{ \sin\left(\frac{2\pi\varepsilon_{\rm F}^2}{(\hbar\omega_{\rm g})^2} \right) + \left(1 - \frac{T/T_{\rm g}^{\rm dHvA}}{\sinh(T/T_{\rm g}^{\rm dHvA})} \right) \frac{1}{2} \cos\left(\frac{2\pi\varepsilon_{\rm F}^2}{(\hbar\omega_{\rm g})^2} \right) \Big/ \frac{2\pi\varepsilon_{\rm F}^2}{(\hbar\omega_{\rm g})^2} \right\} \times \cos^2\left(\sqrt{2} \frac{\varepsilon_{\rm F}}{\hbar\omega_{\rm g}} Kl - \frac{\pi}{4} \right). \quad (22)$$

The above expression accounts for the dHvA-type oscillations in the presence of modulation. At low magnetic fields, the cosine squared term gives rise to new oscillations: Weiss-type oscillations, occurring in ΔF as the amplitude modulation of the dHvA-type oscillations such that zeros result when the electric flat band condition is satisfied. The period of modulation δ is found to be

$$\delta\left(\frac{\sqrt{n_{\rm e}}}{B} \right) = \frac{a}{2\sqrt{2\pi}} \frac{e}{\hbar} \quad (23)$$

which is the same as for the conventional 2DEG system. From equation (22) no temperature scale for the Weiss-type oscillations is obtained. However, if we solve the second integral of equation (17) for $F_{\rm mod}$ by replacing all the energy terms ε by the Fermi energy $\varepsilon_{\rm F}$, except the one which is included in the last cosine function (where small energy changes can influence the damping of Weiss-type oscillations), we find an expression for ΔF containing the temperature scale for the Weiss-type oscillations as well:

$$F_{\rm mod} = \Delta F = \Omega \frac{A}{\pi l^2} (k_{\rm B}T)^2 \frac{\varepsilon_{\rm F}^2}{(\hbar\omega_{\rm g})^2} \cos\left(\frac{2\pi\varepsilon_{\rm F}^2}{(\hbar\omega_{\rm g})^2} \right) \times \int_{-\varepsilon_{\rm F}/2k_{\rm B}T}^{\infty} \ln[1 + \exp(-2\theta)]\, {\rm d}\theta + \Omega \frac{A}{\pi l^2} \frac{\varepsilon_{\rm F}^3}{4\sqrt{2} Kl \hbar\omega_{\rm g}} \cos\left(\frac{2\pi\varepsilon_{\rm F}^2}{(\hbar\omega_{\rm g})^2} \right) - \Omega \frac{A}{\pi l^2} \frac{\varepsilon_{\rm F}^2}{(2\sqrt{2}Kl)^2} \cos\left(\frac{2\pi\varepsilon_{\rm F}^2}{(\hbar\omega_{\rm g})^2} \right) \times \frac{1}{2} \frac{T/T_{\rm g}^{\rm Weiss}}{\sinh(T/T_{\rm g}^{\rm Weiss})} \left\{ 1 + 2\cos^2\left(\sqrt{2} \frac{\varepsilon_{\rm F}}{\hbar\omega_{\rm g}} Kl - \frac{\pi}{4} \right) \right\}, \quad (24)$$

where $T_{\rm g}^{\rm Weiss} = \hbar\omega_{\rm g}/(2\sqrt{2}\pi Klk_{\rm B}) = \frac{\hbar\omega_{\rm g}}{2\pi^2} \frac{a}{2\sqrt{2}lk_{\rm B}}$ defines the critical temperature for the damping of Weiss oscillations in graphene. We can now compare the critical temperature scales for damping of Weiss oscillations in graphene, $T_{\rm g}^{\rm Weiss}$, and conventional 2DEG systems, $T_{\rm 2DEG}^{\rm Weiss}$, where electrons obey the standard parabolic energy spectrum. The critical damping temperature in a conventional 2DEG system [9] is $T_{\rm 2DEG}^{\rm Weiss} = \frac{v_{\rm F}^{\rm p} eBa}{4\pi^2 k_{\rm B}}$, where $v_{\rm F}^{\rm p} = \hbar k_{\rm F}/m_{\rm e}$ is the Fermi velocity of electrons with parabolic energy spectrum and $m_{\rm e}$ is the effective mass of the electron. On comparing the two temperature scales we find that the damping temperature $T_{\rm g}^{\rm Weiss}$ for Weiss oscillations in graphene is higher than $T_{\rm 2DEG}^{\rm Weiss}$ of a 2DEG system. The ratio of critical temperatures of Weiss oscillations is found to be same as that of dHvA-type oscillations:

$$\frac{T_{\rm g}^{\rm Weiss}}{T_{\rm 2DEG}^{\rm Weiss}} = \frac{v_{\rm F}}{v_{\rm F}^{\rm p}} \approx 4, \quad (25)$$

which means a comparatively higher temperature is also required for damping of Weiss-type oscillations in graphene. This is due to the higher Fermi velocity of Dirac electrons in graphene compared to standard electrons in 2DEG systems. From the above discussion, it is evident that both dHvA- and Weiss-type oscillations are more enhanced in the case of graphene. The $\sinh(T/T_{\rm g}^{\rm dHvA})$ factor in the last term of equation (20) is the damping factor with the temperature of dHvA oscillations in graphene. If $T/T_{\rm g}^{\rm dHvA}$ is replaced by $B_{\rm g}^{\rm dHvA}/B$ for graphene and $T/T_{\rm 2DEG}^{\rm dHvA}$ is replaced by $B_{\rm 2DEG}^{\rm dHvA}/B$ for a 2DEG system, where $B_{\rm g}^{\rm dHvA} = 2\pi^2 k_{\rm F} k_{\rm B} T/e v_{\rm F}$ and $B_{\rm 2DEG}^{\rm dHvA} = 2\pi^2 k_{\rm F} k_{\rm B} T/e v_{\rm F}^{\rm p}$ defines the critical magnetic field for graphene and 2DEG, respectively, then we are able to determine the amplitude of dHvA oscillations at a given magnetic field. In figure 6 we have plotted $(\sinh(B_o/B))^{-1}$, where $B_o = B_{\rm g}^{\rm dHvA}$ for graphene and $B_o = B_{\rm 2DEG}^{\rm dHvA}$ for 2DEG systems, respectively, as a function of the magnetic field B at $T = 2$ K. The solid curve is for the graphene system whereas the broken curve is for a conventional 2DEG system. From the figure it can be seen that the curve for the graphene system (solid) leaves the zero axis at a magnetic field of 0.12 T while the curve for the conventional 2DEG system (broken) becomes non-zero at a magnetic field of 0.35 T, depicting minimum values of the magnetic field B for the occurrence of dHvA oscillations for the two systems. These minimum values of critical magnetic fields are consistent with our numerical results. From the values of critical temperature and critical magnetic field B_o, it is clear that conditions favorable for dHvA oscillations in a conventional 2DEG system persists to smaller magnetic fields and higher temperatures in graphene.

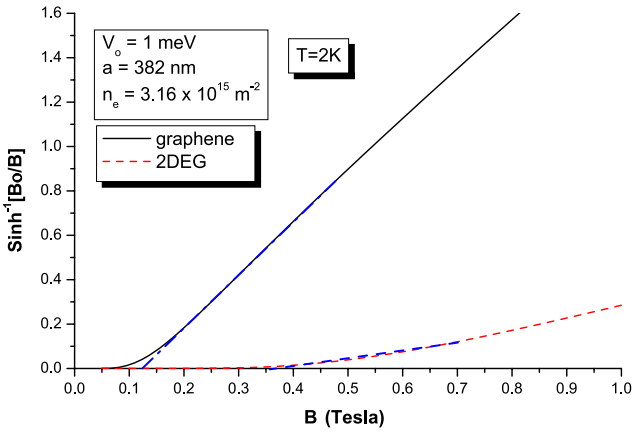

Figure 6. The $(\sinh(B_o/B))^{-1}$ as a function of magnetic field B at $T = 2$ K for graphene system (solid curve) and for conventional 2DEG (broken).

In conclusion, we have presented a study of the thermodynamic properties of a graphene monolayer subjected to a weak electric modulation in the presence of a magnetic field. The results obtained are compared with those of a conventional 2DEG system realized in semiconductor

heterostructures. As a result of the commensurability of two characteristic length scales in the system, period of modulation and cyclotron orbit radius, commensurability oscillations (Weiss type) and dHvA-type oscillations are reflected in all the thermodynamic quantities under consideration in this work for the two systems. However, these effects are more pronounced in a graphene system in the sense that the oscillations in the thermodynamic quantities are more robust against temperature as well as having a higher amplitude than in a conventional 2DEG system. This difference arises due to the different nature of the quasiparticles (Dirac electrons and standard electrons) in the two systems with the result that the energy spectrum for the quasiparticles in the two systems as well as their Fermi velocities are different. On the basis of analytic asymptotic expressions, we are able to determine the critical temperature and critical magnetic field for damping of magnetic oscillations in the thermodynamic properties of an electrically modulated graphene monolayer.

Appendix

Here, we derive the asymptotic expression for the density of states appearing as equation (16) in this paper. We consider a graphene monolayer subjected to a uniform quantizing magnetic field $\mathbf{B} = B\hat{z}$ in the presence of an additional weak periodic modulation potential. The energy spectrum in the quasi-classical approximation when many Landau bands are filled may be written as

$$\varepsilon_{n,x_o} = \sqrt{n}\hbar\omega_g + G(\varepsilon)\cos K x_o \tag{26}$$

where

$$G(\varepsilon) = V_0\pi^{-1/2}\left(\frac{1}{2}K^2l^2\frac{\varepsilon}{\hbar\omega_g}\right)^{-1/4}\cos\left(\sqrt{2}Kl\frac{\varepsilon}{\hbar\omega_g} - \frac{\pi}{4}\right).$$

To obtain a more general result, which will lead to the result that we require as a limiting case, we consider impurity-broadened Landau levels. The self-energy may be expressed as

$$\Sigma^-(\varepsilon) = \Gamma_o^2\sum_n\int_0^a\frac{\mathrm{d}x_o}{a}\frac{1}{\varepsilon - \varepsilon_{n,x_o} - \Sigma^-(\varepsilon)}. \tag{27}$$

Γ_o is the broadening of the levels due to the presence of impurities. The density of states is related to the self-energy through

$$D(\varepsilon) = \mathrm{Im}\left[\frac{\Sigma^-(\varepsilon)}{\pi^2l^2\Gamma_o^2}\right]. \tag{28}$$

The residue theorem has been used to sum the series [18]: $\sum_{-\infty}^{\infty}f(n) = -\{\text{Sum of residues of}\pi(\cot\pi n)f(n)\ \text{at all poles of}\ f(n)\}$. Here $f(n) = \sum_{-\infty}^{\infty}\frac{b}{c-d\sqrt{n}}$ with $b = \Gamma_o^2$, $c = \varepsilon - \Sigma^-(\varepsilon) - G(\varepsilon)\cos Kx_o$ and $d = \hbar\omega_g$. The $f(n)$ has a pole at c^2/d^2 and a residue of $(\pi(\cot\pi n)f(n))$ at the pole is $\frac{-2bc}{d^2}\pi\cot(\frac{\pi c^2}{d^2})$. Hence $\sum_{-\infty}^{\infty}f(n) = \frac{2bc}{d^2}\pi\cot(\frac{\pi c^2}{d^2})$ and we get

$$\Sigma^-(\varepsilon) = \int_0^a\frac{\mathrm{d}x_o}{a}\frac{2\pi\Gamma_o^2(\varepsilon - \Sigma^-(\varepsilon) - G(\varepsilon)\cos Kx_o)}{(\hbar\omega_g)^2} \times \cot\left(\frac{\pi(\varepsilon - \Sigma^-(\varepsilon) - G(\varepsilon)\cos Kx_o)^2}{(\hbar\omega_g)^2}\right) \tag{29}$$

$$\Sigma^-(\varepsilon) \approx \frac{2\pi\Gamma_o^2\varepsilon}{(\hbar\omega_g)^2}\int_0^a\frac{\mathrm{d}x_o}{a}\cot\left(\frac{\pi\varepsilon}{(\hbar\omega_g)^2}[\varepsilon - 2\{\Sigma^-(\varepsilon) + G(\varepsilon)\cos(Kx_o)\}]\right). \tag{30}$$

Separating $\Sigma^-(\varepsilon)$ into real and imaginary parts:

$$\Sigma^-(\varepsilon) = \Delta(\varepsilon) + \mathrm{i}\frac{\Gamma(\varepsilon)}{2}.$$

Equation (27) takes the form

$$\Delta(\varepsilon) + \mathrm{i}\frac{\Gamma(\varepsilon)}{2} = \frac{2\pi\Gamma_o^2\varepsilon}{(\hbar\omega_g)^2}\int_0^a\frac{\mathrm{d}x_o}{a}\frac{\sin u + \mathrm{i}\sinh v}{\cosh v - \cos u} \tag{31}$$

where

$$u = \frac{2\pi\varepsilon}{(\hbar\omega_g)^2}[\varepsilon - 2(\Delta(\varepsilon) + G(\varepsilon)\cos(Kx_o))] \qquad v = \frac{2\pi\varepsilon}{(\hbar\omega_g)^2}\Gamma(\varepsilon). \tag{32}$$

In the case of large collision broadening, $\pi\Gamma \gg \hbar\omega_g$, we can expand with respect to the small quantity $\exp(-v)$ and solve equation (31) by iteration. Up to first order, we obtain

$$\frac{\Gamma(\varepsilon)}{2} = \frac{2\pi\Gamma_o^2\varepsilon}{(\hbar\omega_g)^2}\left[1 + 2\exp\left[-\frac{4\pi^2\varepsilon^2\Gamma_o^2}{(\hbar\omega_g)^4}\right]\cos\left(\frac{2\pi\varepsilon^2}{(\hbar\omega_g)^2}\right) \times\left\{1 - \Omega\varepsilon\cos^2\left(\sqrt{2}\frac{\varepsilon}{\hbar\omega_g}Kl - \frac{\pi}{4}\right)\right\}\right] \tag{33}$$

where

$$\Omega = V^2\frac{a}{l}\left(\frac{\sqrt{2}}{\hbar\omega_g}\right)^3.$$

Using equation (33) in equation (28), an expression for the density of states may be obtained:

$$D(\varepsilon) = \frac{A}{\pi l^2}\frac{2\varepsilon}{(\hbar\omega_g)^2}\left[1 + 2\exp\left[-\frac{4\pi^2\varepsilon^2\Gamma_o^2}{(\hbar\omega_g)^4}\right]\cos\left(\frac{2\pi\varepsilon^2}{(\hbar\omega_g)^2}\right) \times\left\{1 - \Omega\varepsilon\cos^2\left(\sqrt{2}\frac{\varepsilon}{\hbar\omega_g}Kl - \frac{\pi}{4}\right)\right\}\right]. \tag{34}$$

In the limit of vanishing impurity potential, considered in this work, we obtain

$$D(\varepsilon) = \frac{A}{\pi l^2}\frac{\varepsilon}{(\hbar\omega_g)^2}\left[1 + 2\cos\left(\frac{2\pi\varepsilon^2}{(\hbar\omega_g)^2}\right) \times\left\{1 - \Omega\varepsilon\cos^2\left(\sqrt{2}\frac{\varepsilon}{\hbar\omega_g}Kl - \frac{\pi}{4}\right)\right\}\right]. \tag{35}$$

References

[1] Deacon R S, Chuang K C, Nicholas R J, Novoselov K S and Geim A K 2007 *Phys. Rev.* B **76** 081406

[2] Novoselov K S, Geim A K, Morozov S V, Jiang D, Katsnelson M I, Grigorieva I V, Dubonos S V and Firsov A A 2005 *Nature* **438** 197
Zhang Y, Tan Y W, Stormer H L and Kim P 2005 *Nature* **438** 201

[3] Katsnelson M I, Novoselov K S and Geim A K 2006 *Nat. Phys.* **2** 620

Novoselov K S, McCann E, Morozov S V, Fal'ko V I, Katsnelson M I, Zeitler U, Jiang D, Schedin F and Geim A K 2006 *Nat. Phys.* **2** 177
[4] Zhang Y and Ando T 2002 *Phys. Rev.* B **65** 245420
[5] Guysynin V P and Sharapov S G 2005 *Phys. Rev. Lett.* **95** 146801
Perez N M R, Guinea F and Castro Neto A H 2006 *Phys. Rev.* B **73** 125411
[6] Huard B *et al* 2007 *Phys. Rev. Lett.* **98** 236803
Ozyilmaz B *et al* 2007 *Phys. Rev. Lett.* **99** 166804
Williams J R, Di Carlo L and Marcus C M 2007 *Science* **317** 638
Young A F and Kim P 2009 *Nat. Phys.* **5** 222
Stander N *et al* 2009 *Phys. Rev. Lett.* **102** 026807
[7] Weiss D, Klitzing K v, Ploog K and Weimann G 1989 *Europhys. Lett.* **8** 179
Winkler R W, Kotthaus J P and Ploog K 1989 *Phys. Rev. Lett.* **62** 1177
Gerhardts R R, Weiss D and Klitzing K v 1989 *Phys. Rev. Lett.* **62** 1173
Peeters F M and Vasilopoulos P 1993 *Phys. Rev.* B **47** 1466
Shi J, Peeters F M, Edmonds K W and Gallagher B L 2002 *Phys. Rev.* B **66** 035328
Vasilopoulos P and Peeters F M 1990 *Superlatt. Microstruct.* **7** 393
Peeters F M and Matulis A 1993 *Phys. Rev.* B **48** 15166
Xue D P and Xiao G 1992 *Phys. Rev.* B **45** 5986
De Ye P, Weiss D, Gerhardts R R, Seeger M, Klitzing K v, Eberl K and Nickel H 1995 *Phys. Rev. Lett.* **74** 3013
Ho J H, Lai Y H, Chui Y H and Lin M F 2008 *Nanotechnology* **19** 035712
[8] Bai C and Zhang X 2007 *Phys. Rev.* B **76** 075430
Park C-H *et al* 2008 *Nat. Phys.* **4** 213
Barbier M, Peeters F M, Vasilopoulos P and Pereira J M 2008 *Phys. Rev.* B **77** 115446
Park C-H *et al* 2008 *Nano Lett.* **8** 2920
Park C-H *et al* 2008 *Phys. Rev. Lett.* **101** 126804
Brey L and Fertig H A 2009 *Phys. Rev. Lett.* **103** 046809
Brey L and Fertig H A 2009 *Phys. Rev. Lett.* **103** 046808
Park C-H *et al* 2009 *Phys. Rev. Lett.* **103** 046808
[9] Mataulis A and Peeters F M 2007 *Phys. Rev.* B **75** 1254929
Tahir M and Sabeeh K 2008 *Phys. Rev.* B **77** 195421
Ramzani Masir M, Vasilopoulos P and Peeters F M 2009 *Phys. Rev.* B **79** 035409
Dell'Anna L and De Martino A 2009 *Phys. Rev.* B **79** 045420
Ghosh S and Sharma M 2009 *J. Phys.: Condens. Matter* **21** 292204
Snyman I 2009 *Phys. Rev.* B **80** 054303
[10] Pletikosic I, Kralj M, Pervan P, Brako R, Coraux J, Diaye A T Ń, Busse C and Michely T 2009 *Phys. Rev. Lett.* **102** 056808
Marchini S, Gunther S and Wintterlin J 2007 *Phys. Rev.* B **76** 075429
Vazquez de Parga A L *et al* 2007 *Phys. Rev. Lett.* **100** 056807
Pan Y *et al* 2007 arXiv:0709.2858 [cond-mat]
[11] Meyer J C *et al* 2008 *Appl. Phys. Lett.* **92** 123110
[12] Brey L and Palacios J J 2008 *Phys. Rev.* B **77** 041403(R)
Isacsson A *et al* 2008 *Phys. Rev.* B **77** 035423
[13] Stewart S M and Zhang C 1998 *J. Phys.: Condens. Matter* **10** 5545
[14] Peeters F M and Vasilopoulous P 1992 *Phys. Rev.* B **46** 4667
[15] Gradshteyn I S and Ryzhik I M 1994 *Tables of Integrals, Series, and Products* (New York: Academic)
[16] Tahir M, Sabeeh K and Mackinnon A 2007 *J. Phys.: Condens. Matter* **19** 406226
[17] Patheria R K 1996 *Statistical Mechanics* (Oxford: Butterworth–HeineMann)
[18] Spiegel M R 1964 *Theory and Problems of Complex Variables* (*Schaum's Outline Series*) (New York: McGraw-Hill)
[19] Ohta T *et al* 2006 *Science* **313** 951
Ohta T *et al* 2007 *Phys. Rev. Lett.* **98** 206802
Zhou S Y *et al* 2007 *Nat. Mater.* **6** 770
Riedl C *et al* 2008 *Appl. Phys. Lett.* **93** 033106
Bostwick A *et al* 2007 *Nat. Phys.* **3** 36
Giovannetti G *et al* 2008 *Phys. Rev. Lett.* **101** 026803